Nano-scale characterisation of tri-modal microstructures in TIMETAL® 575

Enrique Frutos-Myro[1]*, Ian MacLaren[2], Peifeng Li[1], Iain Berment-Parr[3], Mathew Thomas[3]
[1]School of Engineering, University of Glasgow, Glasgow, G12 8QQ, UK
[2]School of Physics and Astronomy, University of Glasgow, Glasgow, G12 8QQ, UK
[3]Timet UK ltd, PO Box 704, Witton, Birmingham, B6 7UR, UK
*e.frutos-myro.1@research.gla.ac.uk

Abstract
TIMETAL® 575, developed by Titanium Metals Corporation (TIMET), is a high strength forgeable α+β titanium alloy with comparable density, beta transus temperature and processing characteristics to Ti-6Al-4V but with enhanced static and fatigue strength primarily aimed at aero-engine disc or blade applications. Recent research on this alloy has focussed on microstructure evolution as a means to optimise mechanical behaviour and it has been concluded that a solution heat treatment followed by an ageing step yields a resulting "tri-modal" microstructure, consisting of equiaxed primary α and bi-lamellar transformation product containing nano-scale "tertiary alpha" laths, which appear to provide an excellent balance of strength and ductility. The key objective of the work presented here is to characterise this complex nanoscale microstructure in detail at various stages of alloy processing. For that purpose various advanced and recently developed transmission electron microscopy (TEM) techniques have been used. These include alpha and beta phase mapping Precession Electron Diffraction (PED), overall microstructure imaging with conventional BF and DF TEM, distinction of fine phase detail with high angle annular dark field (HAADF) scanning TEM (STEM), and correlation of the nanostructure to the elemental distribution using scanned Electron Energy Loss Spectroscopy (EELS).

Introduction
Titanium alloys can be engineered to have a range of desirable properties and as such they are widely used in several areas such as medicine, chemistry, architecture and transportation [1]. However, the aerospace industry has become the main consumer of titanium due to its high strength to weight ratio, low density and excellent corrosion resistance [2][3]. For gas turbine applications α+β alloys, in particular Ti-6Al-4V, and near α alloys have seen extensive use in the fan and compressor stages. Nevertheless, new alloy compositions and thermo-mechanical processing routes have been developed in order to improve component performance [3][4].
In relation to the thermo-mechanical processing, some authors have reported methods by which a lamellar microstructure could be processed into a bi-lamellar microstructure consisting of nano-scale α plates within the β lamellae. Examples of alloys processed to produce this microstructure are Ti-6242 and Ti-6Al-4V reported by Lutjering [5]. The same method was then proposed for modifying alloys with bi-modal starting microstructure in order to produce a 'tri-modal' microstructure which would consist of equiaxed primary α grains (αp) and secondary α laths (αs) as well as nano-scale

tertiary α plates (αt) found within the remaining β matrix [6].
TIMETAL® 575 (Ti-575), developed by TIMET, is a high strength forgeable α+β titanium alloy with comparable density, beta transus temperature and processing characteristics to Ti-6Al-4V but with enhanced static and fatigue strength primarily aimed at aero-engine disc or blade applications. Research into the microstructural evolution of this alloy has been performed with the aim of improving and optimising the mechanical behaviour and it has been determined that a solution heat treatment followed by an ageing step resulted in an optimised 'tri-modal' microstructure consistent with those previously described by Lutjering, which appear to provide an excellent balance of mechanical properties [7][8][9][10].
The main objective of the work presented here is to characterise nano-scale microstructure of Ti-575 after various stages of processing in order to investigate the development and corroborate the presence of a tri-modal structure.

Experimental procedures

The nominal composition of Ti-575 in mass percent is Ti-5.3Al-7.7V-0.25Fe-0.5Si-0.18O. Its density and β transus values have been reported as 4.47 g/cm3 and 965 oC, respectively [11].
The Ti-575 used in this study was manufactured by TIMET UK ltd. A triple melted vacuum arc remelt (VAR) ingot was forged on production equipment using a proprietary sequence of ingot breakdown and billet forging in order to produce a bi-modal equiaxed α+β billet microstructure. Billet slices were removed for further processing at the laboratory scale. The slices were pancake forged below the β transus and then solution heat treated with a controlled cooling rate to optimise the microstructure. Either an anneal (700oC for 2 hours) or an age (500oC for 8 hours) was then applied to produce different αt content. These processing steps are schematically illustrated in Figure 1 [9] [11].

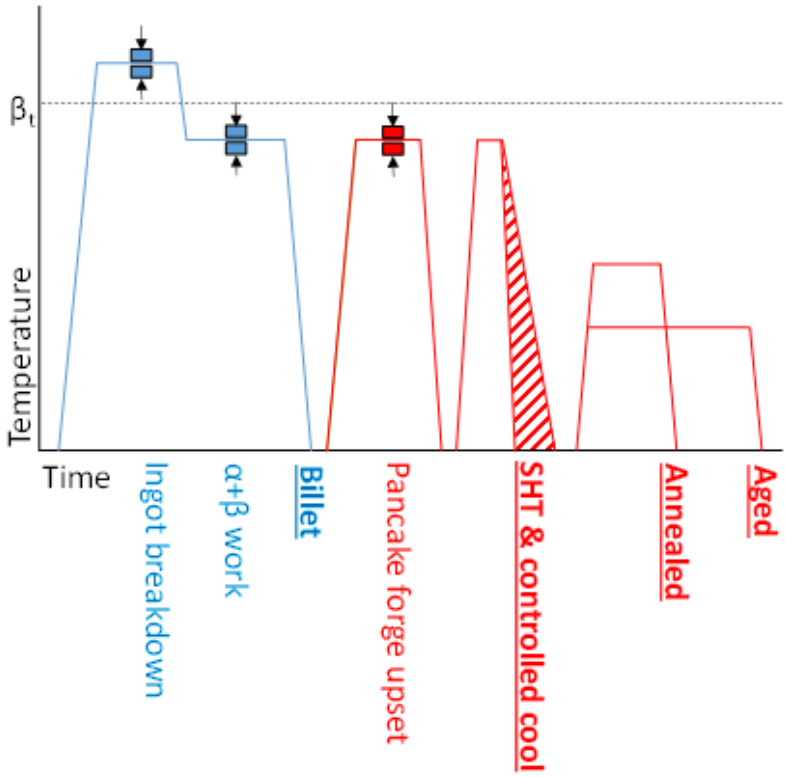

Figure 1. Schematic representation of the processing route for TIMETAL®575 alloy samples. The blue section shows steps undertaken by production forging of full-scale ingot to billet, whilst the red secion shows laboratory scale research steps using billet slices.

One sample in the as-forged billet, solution heat treated, annealed and aged condition was taken and prepared to determine the microstructural evolution at each of these four points during processing. The samples were ground and polished following standard metallographic methods. In order to characterise the microstructure of this alloy, Scanning Electron Microscopy (SEM) in Backscattered Electron mode (BSE) by using a Concentric Backscatter detector (CBS) was conducted using a Helios Plasma Focused Ion Beam (PFIB) system which includes a xenon plasma ion beam column and a FEG-SEM column at 52o to the ion column. Samples for Transmission Electron Microscopy (TEM) were prepared using either a Dual Beam Focused Ion Beam (FIB) or the PFIB systems using a standard lift out procedure. TEM characterisation was conducted using a FEI Tecnai T20 microscope.

Results and discussions

Scanning Electron Microscopy

As illustrated in Figure 1, the development of a tri-modal microstructure has been investigated at four points during the thermo-mechanical processing of Ti-575. A representative image of the bulk microstructure at each point is shown in Figure 2.

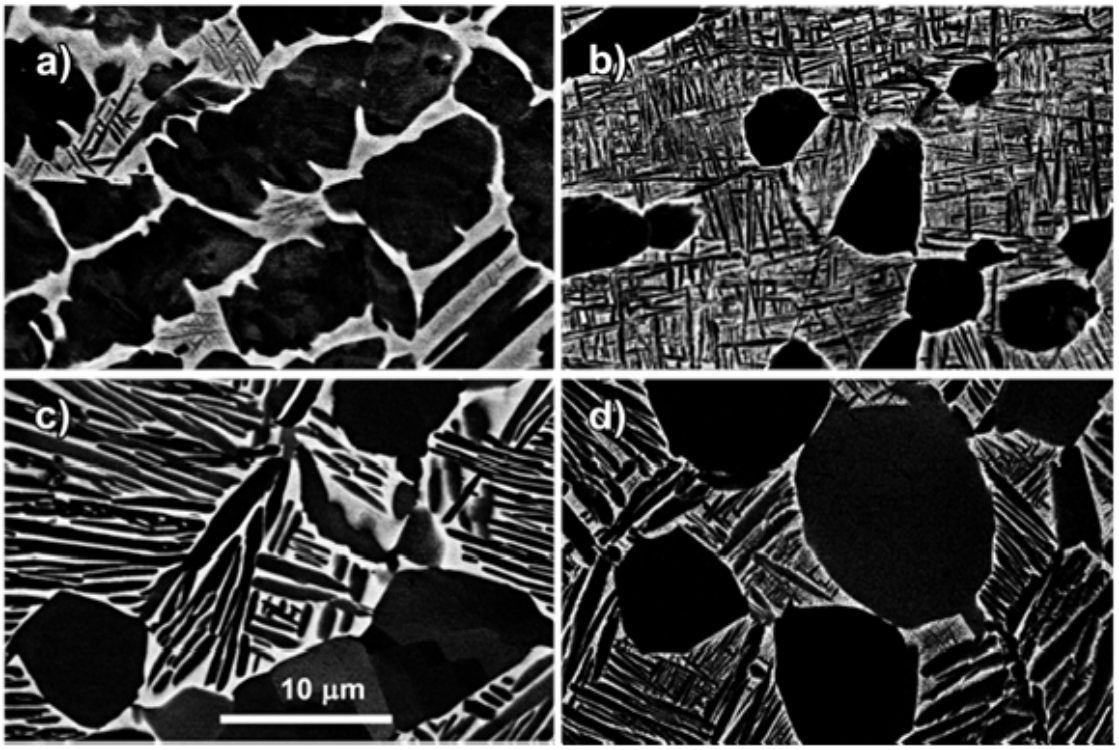

Figure 2. SEM BSE images of the four samples, where β is the bright phase, and α is the dark phase, for (a) as-forged billet sample; (b) solution heat treated and fan air cooled sample; (c) annealed sample; and (d) aged sample. Equiaxed αp grains are observed at all stages, however, the αs lamella in the β matrix differs with heat treatment. The same scale bar applies for all images.

From Figure 2 it can be seen that the morphology of the different features in the billet microstructure are drastically modified with thermo-mechanical processing; through pancake forging and solution heat treatment it can be seen that the αp grains reduce in area fraction and become more globular. The width and density of the αs laths is a function of the controlled cooling rate from solution heat treatment. The most significant difference between the subsequently aged and annealed samples is the presence (or absence) of the nano-scale αt plates within the β lamellae as can be seen in Figure 3. The αt is not homogeneously distributed and appears more abundant in some areas. Specifically, the αt mainly tends to form near the αp grains and within wider transformed β regions.

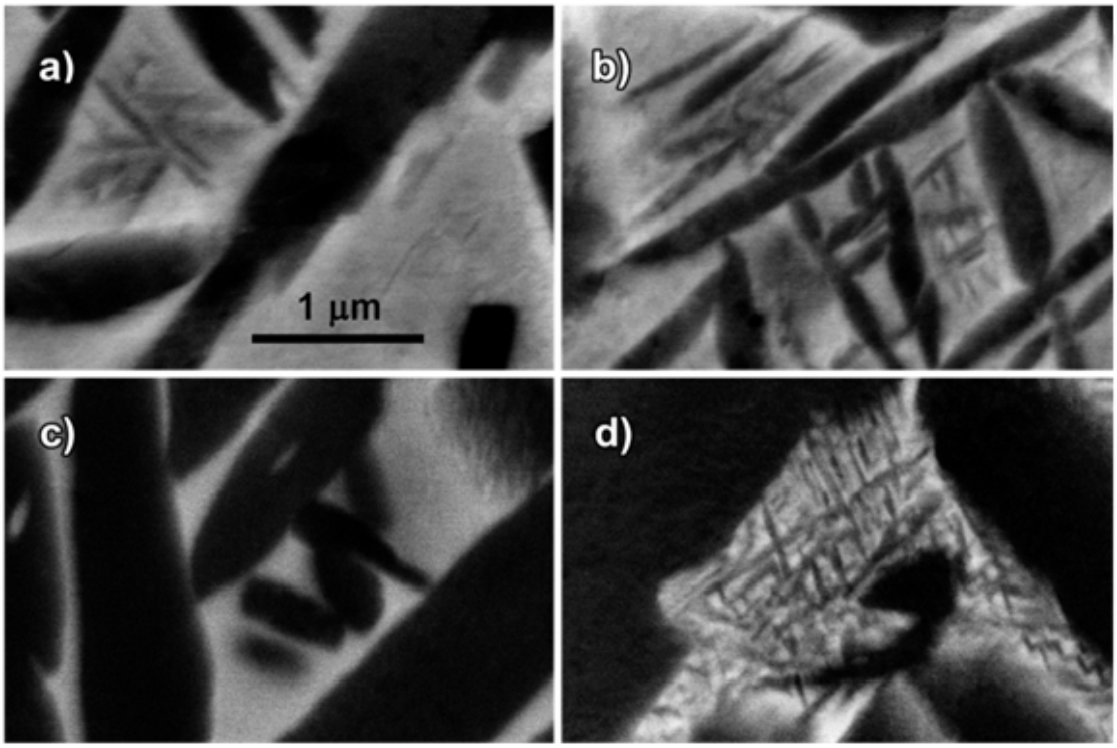

Figure 3. Higher magnification SEM BSE images of β areas of Ti-575, where β is the bright phase, and α is the dark phase: (a) billet containing some limited nano-scale αt; (b) solution heat treated material containing some αt between the αs laths; (c) annealed material without any nano-scale αt; and (d) aged material containing large number of densely packed nano-scale αt between the αs laths. The same scale bar applies for all images.

In Table 1 an attempt has been made to quantify the proportions of each phase within the microstructure for each of the four points during processing. Image analysis tools have been used to estimate the average area fraction of αt across a number of high magnifications images and this has been subtracted from the observed αs+β content in lower magnification images.

Table 1. Phase quantification of TIMETAL® 575 microstructure at each stage of processing.

	Billet	As-solution heat	As-annealed	As-aged

		treated		
Area fraction α_p (%)	60	19	18	20
Estimated area fraction $\alpha_s+\beta$ (%)	37	77	82	72
Estimated area fraction α_t (%)	3	4	-	8

Transmission Electron Microscopy

a) Characterisation by Transmission Electron Microscopy

In order to characterise the microstructure in finer detail it is necessary to overcome the maximum resolution that can be achieved within the SEM by moving to TEM imaging techniques. Within the TEM, a first study on the crystallographic orientation and the chemical composition of the αt phase has been conducted.

In the dark field image of the as-forged Ti-575 billet shown in Figure 4a a region containing both αs and αt laths can be seen. In Figure 4b, a dark field condition is set up that highlights a group of several αs laths. Figure 4c at a different dark field condition highlights a group of parallel αt laths as bright, indicating they all have similar crystallographic orientation. Because their brightness varies with different orientations of the dark field tilt, it can be concluded that the αs laths have a different orientation to the adjacent αt laths present in the field of view. With regard to the β phase, all regions were shown to have the same contrast, showing that both the αs and αt laths (shown together in Figure 4d) have transformed from within the same β grain.

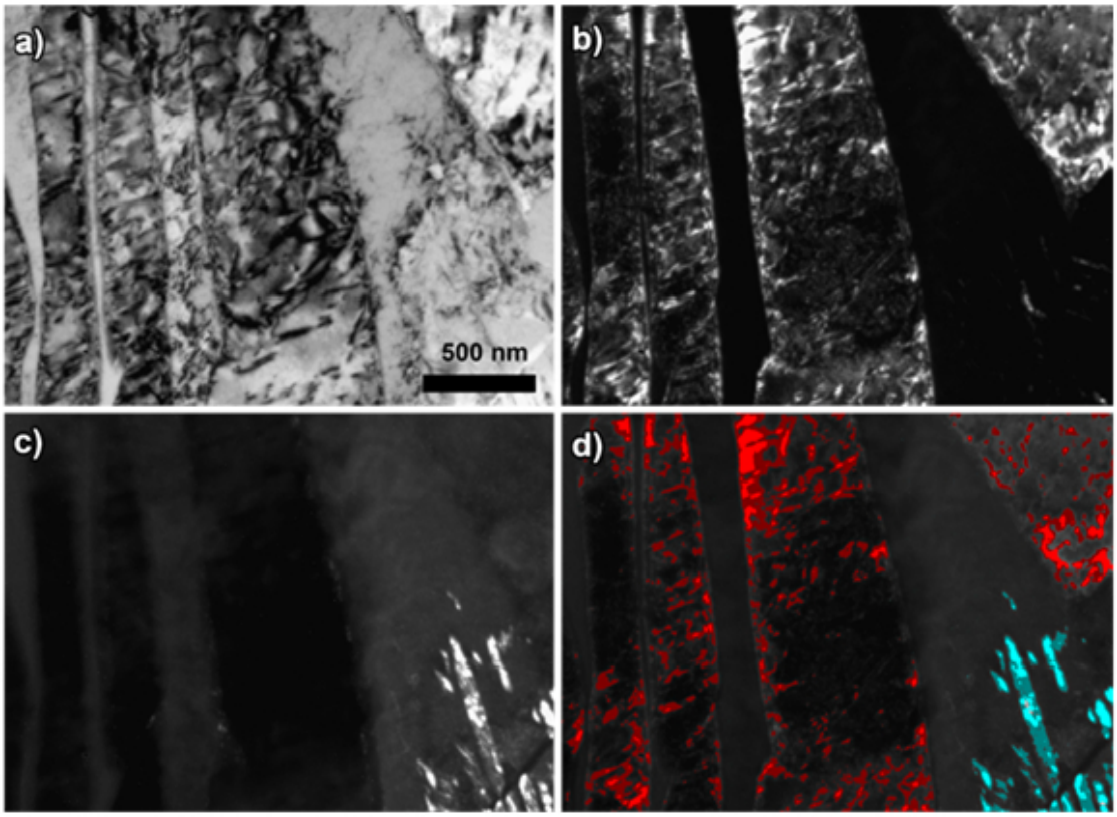

Figure 4. a) Bright field image of the TIMETAL® 575 billet; (b) Dark field image highlighting several αs laths with the same crystal orientation as bright, the β phase is dark; (c) Dark field image showing bright αt laths, the β phase is grey and the αs laths are dark; and (d) RGB image highlighting αs laths in red, αt laths in blue.

b) Scanning Precession Electron Diffraction (SPED)

It is possible in a transmission microscope to obtain pseudokinematic electron diffraction patterns by precessing the beam around the optic axis of the microscope [12]. When the precessed beam is scanned across the sample it can provide, in relatively little time and quite accurately, maps of the crystallographic phase and orientation as a function of position using a pattern matching algorithm [13]. Recent work on integrating SPED with a newer electron counting detector [14] is increasing speed and reducing noise in scans. For the present application, this provides a more straightforward way of distinguishing α and β phases and mapping their orientations over larger areas than is possible with conventional dark field TEM imaging.

Figure 5 shows a set of maps derived from one SPED dataset. Figure 5a shows an orientation reliability map from SPED analysis of Ti-575 in an as-forged condition; laths and areas between laths are clearly recognised as brighter areas, whereas boundaries are dark (probably because there are pattern overlaps leading to a difficulty in indexing). Figure 5b shows a phase identification map where α is red and β is green (with the image quality superimposed to suppress noisy or unreliable pixels at boundaries); it is clearly seen that mapping large areas with high reliability is straightforward, and with more detail than is possible using backscattered electrons in the SEM, as seen in Figure 3. Figure 5c and 5d are orientation colour maps relative to the x direction for the α and β phases, respectively. These corroborate the findings of the standard TEM results, but in a similar way to EBSD in the SEM, show a larger set of quantitative crystallographic orientation data in a simple colour scale image. Figure 5c shows that the coarse αs laths already have a number of different orientations, including those represented by greenish, yellowish, pink and aqua colours. Additional colours appear in the tight nest of nano-scale αt laths in the centre, showing more crystal orientations, and demonstrating that many different orientations are nucleated simultaneously in the formation of the αt. It should also be noted that using this colour scale to just represent the x orientation means some inequivalent orientations produce similar colours, so differently oriented laths probably have a different crystal orientation, even if a similar colour is seen in this representation. Conversely, Figure 5d shows that the β phase appears to be in the same orientation across this entire area, with just small changes in shade indicating some sample bending after thinning in response to internal stress, as indicated by the area coloured consistently in a range of purplish shades.

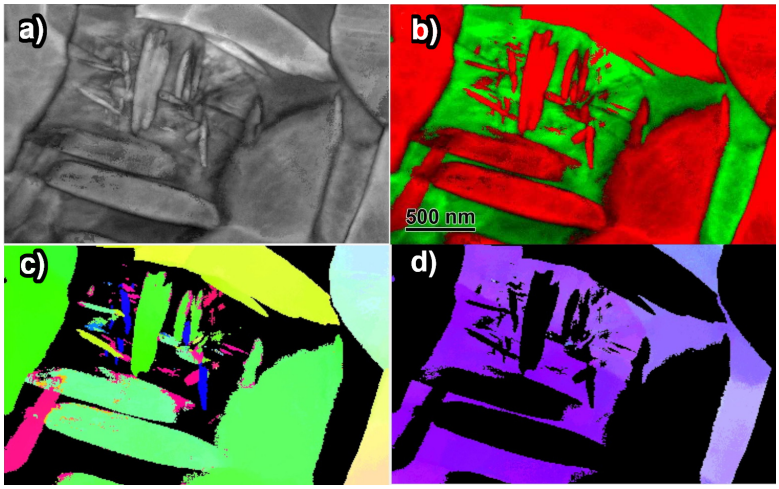

Figure 5. SPED maps of as-forged TIMETAL® 575: a) orientation reliability map ; b) phase map (α in red and β in green) overlaid on the pattern match index (greyscale), bright colours mean high certainty about indexing and darker colours indicate boundaries or defects that

degrade diffraction pattern quality; c) map of the x axis orientation in the α phase only (β phase black); d) map of the x axis orientation for β phase only (α phase black).

c) Electron Energy Loss Spectroscopy (EELS)

Attempts have been made to analyse the nano-scale chemical composition of Ti-575 and particularly the difference in composition between the features present in the microstructure. The main alloying elements of this alloy are vanadium and aluminium which can be classified as β and α stabilisers respectively [3]. As expected, it can be seen from the EELS spectrum in Figure 6 that vanadium is mainly present within β lamellae. Aluminium was found to be located within the αs and αt laths.

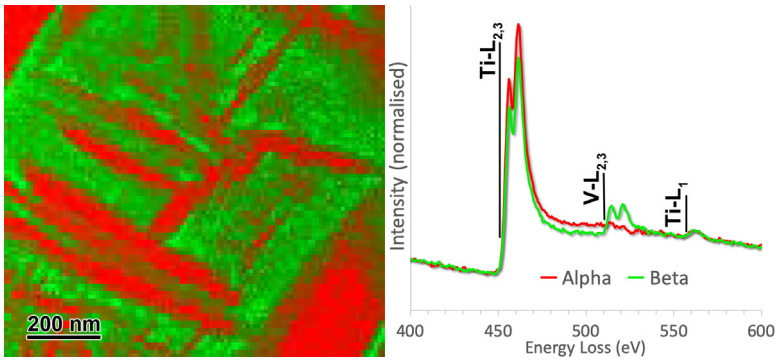

Figure 6. Image (left) of a cluster of αt laths from fitting an EELS spectrum (right) as sum of spectra showing a vanadium peak typical of β (green) and spectra showing no vanadium peak typical of α (red).

However, more work is necessary in order to characterise variations in chemical composition in more detail. It is expected that subtle variations in the chemical composition of each of the α phases will be present due to αp, αs and αt laths forming at different stages of alloy processing.

Conclusions and future work

In this work, nano-scale characterisation of four different points in the processing and heat treatment of Ti-575 has been presented. It has been confirmed that a solution heat treatment followed by a 500oC, 8 hour ageing step resulted in a 'tri-modal' microstructure consisting of αp grains, αs laths and transformed β containing nano-scale αt laths. Notably, some αt phase is also present in smaller quantities in the billet and solution heat treated condition, but not after annealing at 700oC for 2 hours.

The origin of these nano-scale αt laths is still unclear. As previously mentioned in the introduction, no specific chemical composition or processing criteria have clearly been defined for their occurrence in the academic literature. Further detailed characterisation of samples in various thermo-mechanical

processing conditions is required to fully understand their formation and influence on mechanical properties. Particular focus should be on identifying any subtle chemical or crystallographic characteristics that may point towards a particular mechanism for nucleation of the αt phase under the specific processing conditions where it has been observed.

References

[1] C. Leyens, M. Peters, Titanium and titanium alloys: fundamentals and applications. John Wiley, 2003.
[2] R. R. Boyer, Mater. Sci. Eng. A. 213 (1996) 103-114.
[3] G. Lutjering, J. C. Williams, Titanium (Engineering Material and Processes). Springer, 2007.
[4] A. Mouritz, Introduction to aerospace materials. Cambridge: Woodhead, 2012.
[5] G. Lutjering, Mater. Sci. Eng. A. 243 (1998) 32-45.
[6] Y. Chong, N. Tsuji, T. Bhattacharjee, Proceedings of the 13th World Conference on Titanium. (2016) 663-668.
[7] M. Thomas, J. Hewitt, M. Bache, R. Thomas, P. Garratt, Y. Kosaka, Proceedings of the 13th World Conference on Titanium. (2016) 979-984.
[8] J. S. Hewitt, M. J. Thomas, P. Garratt, M. R. Bache, Advanced Materials Research. 891-892 (2014) 569-574.
[9] J. S. Hewitt, P. D. Davies, M. J. Thomas, P. Garratt, M. R. Bache, Mater. Sci. Technol. 30 (2014) 1919-1924.
[10] Y. Millet, S. Andrieu, I. von Thungen, A. Lenain, Proceedings of the 13th World Conference on Titanium. (2016) 1543-1546.
[11] M. Thomas, J. Hewitt, M. Bache, R. Thomas, P. Garratt, Y. Kosaka, Proceedings of the 13th World Conference on Titanium. (2016) 1537-1541.
[12] A. S. Eggeman, P. A. Midgley, Advances in Imaging and Electron Physics. 170 (2012) 1-272.
[13] E. F. Rauch, J. Portillo, S. Nicolopoulos, D. Bultreys, S. Rouvimov, P. Z. Moeck, Krist.-Cryst. Mater. 225 (2-3) (2010) 103-109.
[14] J. A. Mir, R. Clough, R. MacInnes, C. Gough, R. Plackett, I. Shipsey, H. Sawada, I. MacLaren, R. Ballabriga, D. Maneuski, V. O'Shea, D. McGrouther, A. I. Kirkland, Ultramicroscopy 182 (2017) 44-53.